

## EFFECT OF BAROCLINIC CIRCULATION ON THE TRANSPORT OF CONSOLIDATED SEDIMENTS

Wahyu W. Pandoe and Billy L. Edge, Department of Civil Engineering, Texas A&M University, College Station, Texas, USA.

### ABSTRACT

The objective of this research is to identify the circulation patterns of the water and distribution of sediment concentration in Galveston Bay. The fresh water inflow from San Jacinto and Trinity Rivers into the bay carrying high sediment concentration was predicted to contribute to shoaling process in the bay, especially in the ship channel. The three-dimensional finite element numerical model with baroclinic term used in this study provides general characteristics of sediment transport in the Bay. The understanding of these processes can provide a basis for determining how the three-dimensional circulation controls the hydrodynamics of the system and ultimately the transport of suspended material.

### RESUME

L'objectif de cette recherche est d'identifier le comportement de l'écoulement (ou la circulation) de l'eau ainsi que la distribution de la concentration en sédiments dans la baie de Galveston. Le courant d'eau douce provenant des rivières San Jacinto et Trinity et se jetant dans la baie tout en transportant une concentration élevée en sédiments a été prédit pour prendre en compte le processus de création de bancs de sable dans la baie, tout particulièrement dans le canal (servant au passages des bateaux). Le modèle numérique en 3 dimensions par la méthode des éléments finis utilise dans cette étude, fournit les caractéristiques générales du transport de sédiments la baie. La compréhension de tels procédé peut servir de base pour déterminer la manière dont l'écoulement de l'eau contrôle l'hydrodynamique de ce système et finalement, le transport des matériaux en suspension.

### 1. INTRODUCTION

This work provides a general hydrodynamic circulation model that can be used in the development of density driven flows which may arise in the case of suspension of fine-grained materials. The model will be used in pursuit of specific, focused engineering and scientific investigations in Galveston Bay, Texas (Figure 1).

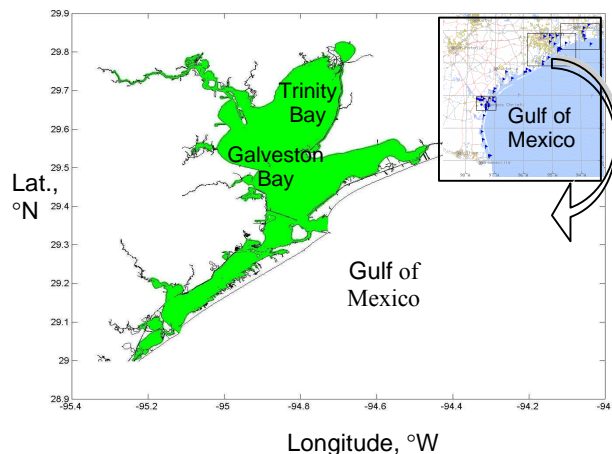


Figure 1. Study area of Galveston Bay and adjacent Trinity Bay located in the Texas coast of Gulf of Mexico (inset).

Galveston Bay is approximately 18km long and 10km wide, and 2 to 4 meters deep. The Galveston Bay system gets an

outflow of fresh water from various sources. Bay waters get fresh water mainly from San Jacinto and Trinity Rivers, and saline waters from Gulf currents and tides; therefore salinity and temperature vary spatially and temporally. Those two rivers contribute about 82% of the total bay system inflow (GBNEP, 1994). Inflow into the Galveston Bay from the Gulf of Mexico comes from two major inlets and one minor cut: (1) "Bolivar Roads" is the main inlet to the bay that provides 80% of the tidal exchange between the Bay System and the Gulf. (2) San Luis Pass is located between the west end of Galveston Island. (3) "Rollover Pass" located at the eastern most part of East Bay is a small channel cut responsible for minor amounts of tidal exchange.

Shoaling process in the bay is presumed to correlate with the flow pattern inside the Bay driven by tide generating current. Sediment conveyed by river runoff from surrounding river inlets might also be one of the sedimentation sources. Long-term shoaling tends to cover sediments that may be contaminated and if left unmoved may provide adequate remediation. However, in episodic conditions, significant energy can erode the cover layer creating exposure to the underlying sediments.

### 2. MODEL DESCRIPTION

The equation of motion shows that water moves in response of differences in pressure, which is generated by two factors: water surface slope and horizontal water density differences. The former is called *barotropic* where a flow is defined as that state of fluid for which density ( $\rho$ ) is a function of only the pressure, and the latter is called

*baroclinic* flow where the water motion driven by differences in density. This type of flow can be established due to changes in the density gradient. Water density is typically related to the salinity and temperature of surrounding water. However when large amounts of sediment are suspended, they too may contribute to the baroclinic conditions.

The scope of this research is to implement and expand the hydrodynamic numerical modeling system to accommodate these density driven flows for Galveston Bay. The model used here is an extension of the Advanced Circulation Model (ADCIRC) originally developed by University of North Carolina in early 1990's (Luettich et al., 1992). ADCIRC is a two and three dimensional depth integrated finite element model used for hydrodynamic circulation problems. The model is based on the finite element codes that solve the shallow water equation on unstructured grids. The finite element formulation has the advantage of flexibility in resolution over the area domain. Fine resolution can be specified locally to meet the accuracy requirements, and coarse resolution can be implemented in area distant from the region of interest.

The computation of hydrodynamics is performed in a bottom and surface-following "s" coordinate system, in which  $\sigma = 1$  at the free surface and  $\sigma = -1$  at the bottom. Two-dimensional ADCIRC models have been successfully implemented for estuaries, tidal inlets, navigation channel, harbor bay, and many other cases of dynamic circulation. For the three-dimensional model, the computed vertical velocity contributes a significant added value to the fall velocity of fine-grained sediments (Pandoe & Edge, 2003). The 3D model includes the second moment turbulence closure scheme of Mellor and Yamada (1982) to provide vertical mixing coefficients.

The governing equations for ADCIRC-3D are given as follows:

continuity equation

$$\frac{\partial \eta}{\partial t} + \frac{\partial uH}{\partial x} + \frac{\partial vH}{\partial y} + (a-b) \frac{\partial \eta}{\partial s} = 0 \quad [1]$$

momentum equations in the longitudinal and lateral directions:

$$\begin{aligned} \frac{\partial u}{\partial t} + u \frac{\partial u}{\partial x} + v \frac{\partial u}{\partial y} + \left( \frac{a-b}{H} \right) \frac{\partial u}{\partial s} - fv = \\ -g \frac{\partial \eta}{\partial x} + m_{x\sigma} - b_{x\sigma} + \left( \frac{a-b}{H} \right) \frac{\partial}{\partial s} \left( \frac{t_{zx}}{\rho_0} \right) \end{aligned} \quad [2]$$

$$\begin{aligned} \frac{\partial v}{\partial t} + u \frac{\partial v}{\partial x} + v \frac{\partial v}{\partial y} + \left( \frac{a-b}{H} \right) \frac{\partial v}{\partial s} + fu = \\ -g \frac{\partial \eta}{\partial y} + m_{y\sigma} - b_{y\sigma} + \left( \frac{a-b}{H} \right) \frac{\partial}{\partial s} \left( \frac{T_{zy}}{\rho_0} \right) \end{aligned} \quad [3]$$

where  $u$  and  $v$  are velocities in the  $x$  and  $y$  direction;  $\omega$  = vertical velocity in  $\sigma$ -coordinate;  $f$  = Coriolis force;  $g$  = gravity acceleration;  $\eta$  = free surface elevation;  $m_{x\sigma}$  = combined horizontal diffusion/dispersion momentum;  $b_{x\sigma}$  and  $b_{y\sigma}$  = baroclinic pressure term in  $x$ - and  $y$ -directions;  $\tau_{zx}$  and  $\tau_{zy}$  = component of vertical shear stress; and  $\rho_0$  = reference density of water.

The solution strategy for horizontal velocities  $u$  and  $v$  involves replacing the velocities with shear stress as the dependent variables, and is then developed by discretizing the shear stress equation, later called *direct stress solution* (DSS). The detail of the 3D DSS formulations is given in Luettich et al. (1994). Once  $\tau_{zx}$  and  $\tau_{zy}$  are determined, velocity can be obtained by:

$$u(s) = u_b + \frac{H}{(a-b)} \int_b^s \frac{t_{zx}}{E_z \rho_0} ds \quad [4]$$

$$v(s) = v_b + \frac{H}{(a-b)} \int_b^s \frac{t_{zy}}{E_z \rho_0} ds \quad [5]$$

where  $u_b$  and  $v_b$  are the components of bottom slip velocities.

Vertical velocity is solved by the first derivative approach with the adjoint correction. Pandoe and Edge (2003) solved for  $w$  in  $s$ -coordinate, with essential boundary condition  $w = 0$  at  $s = b$ , and natural boundary condition  $dw/ds = 0$  at  $s = a$ :

$$\tau_{k+1} - \tau_k = -\frac{1}{(a-b)} \int_k^{k+1} \left( \frac{\partial \tau}{\partial t} + \frac{\partial(uH)}{\partial x} + \frac{\partial(vH)}{\partial y} \right) ds \quad [6]$$

where  $k$  is a node number over vertical element. The solution  $w_k$  will satisfy the bottom boundary condition only. In order to satisfy the free surface, the adjoint correction is applied based on Luettich and Muccino (2001) and Muccino et al. (1997):

$$\tau_{adj} = \tau_s - \tau_s \left( \frac{(s-b) + \frac{HL}{a-b}}{(a-b) + \frac{2HL}{a-b}} \right) \quad [7]$$

where  $w_s(\mathbf{h})$  is the misfit of surface boundary condition at the free surface  $\mathbf{h}$ , and  $L$  is the weight of the relative contribution of the boundary conditions versus the interior solution. The value  $L=0$  is applied to the resulting  $w_s$  which is equal to adding a linear correction to the 1<sup>st</sup> order derivative equation that satisfies only the bottom boundary condition ( $w_s = 0$  at  $s = b$ ). This adjoint correction will give the solution exactly at the surface boundary condition, which in this case  $w_{adj} = 0$  at  $s = a$ .

The governing equations for transport of salinity, temperature and concentration (Mellor, 1998; Scheffner, 1999; and HydroQual, 1998) are summarized as:

$$\frac{\partial C}{\partial t} + u \frac{\partial C}{\partial x} + v \frac{\partial C}{\partial y} + \frac{(a-b)}{H} (\omega - \omega_s) \frac{\partial C}{\partial s} = \quad [8]$$

$$\frac{\partial}{\partial x} \left( D_h \frac{\partial C}{\partial x} \right) + \frac{\partial}{\partial y} \left( D_h \frac{\partial C}{\partial y} \right) + \left( \frac{a-b}{H} \right)^2 \frac{\partial}{\partial s} \left[ D_v \frac{\partial C}{\partial s} \right] + SS$$

where SS is the source/sink terms; C represents salinity [psu], temperature [°C] or sediment concentration [g/l];  $D_h$  and  $D_v$  = horizontal and vertical dispersion coefficients [ $m^2 s^{-1}$ ];  $\omega$  = vertical velocities in  $\sigma$ -coordinate [m/s];  $\omega_s$  = settling velocity of sediment in  $\sigma$ -coordinate [m/s];

For salinity simulation,  $\omega_s$  and SS terms are set to zero. For temperature simulation,  $\omega_s = 0$ , while SS term and surface boundary condition are given as:

$$SS = \frac{(a-b) Q_{ps}}{\rho_o C_p H} \quad [9a]$$

$$\left( \frac{a-b}{H} \right) \left( D_v \frac{\partial T}{\partial s} \right) = \frac{Q_{ns}}{\rho_o C_p} \quad \text{at } z \rightarrow \eta \quad [9b]$$

and for sediment concentration simulation:

$$SS = E - D \quad \text{at } z \rightarrow -h \quad [10]$$

where  $C_p$  is the specific heat of sea water [J/kg/°C] given as:  $C_p \approx 3.94 \times 10^3$  J/kg/°C;  $Q_{ns}$  [W/m<sup>2</sup>] is the net surface heat flux; and  $Q_{ps}$  is the heat loss by solar radiation penetrating the water layer; varies with depth [W/m<sup>2</sup>]; given in Hayes et al. (1991):

$$Q_{pen} = 0.45 Q_{short} \exp(-\gamma h) \quad [11]$$

with  $Q_{short}$  = a short wave surface heat flux from the atmosphere, and its mean value is about 250 W/m<sup>2</sup>; the exponential decay coefficient  $\gamma = 0.04 m^{-1}$  and  $h$  is the layer depth.; E and D represent erosion and deposition flux of sediment, respectively.

The baroclinic terms  $b_{x\sigma}$  and  $b_{y\sigma}$  in Eqs. (2) and (3) are a function of density distribution. The variable density is determined from temperature T, salinity S and pressure p using the International Equation of State of Sea Water, IES80.

$$\rho(S, T, p) = \frac{\rho(S, T, 0)}{1 - \frac{p}{K(S, T, p)}} \quad [12]$$

For each combination of these variables, the density of the sea water is asserted therefore to be uniquely specified. The values of  $\rho(S, T, 0)$  and  $K(S, T, p)$  depend upon the fundamental variables T, S and p. Values are given in Fofonoff (1985). The normalized density  $\rho$  may be separated into two portions – one from the potential temperature and salinity,  $\rho_N$ , and one from the pressure,  $\rho_P$ . Treating sound velocity c as a constant yields cancellation

of pressure term (Robertson, 2001), and then the baroclinic terms can be written as:

$$b_{x_s} = gH \int_s^a \left[ \frac{\partial \rho_N}{\partial x} - \frac{(a-b)s}{H} \frac{\partial H}{\partial x} \frac{\partial \rho_N}{\partial s} \right] ds \quad [13a]$$

$$b_{y_s} = gH \int_s^a \left[ \frac{\partial \rho_N}{\partial y} - \frac{(a-b)s}{H} \frac{\partial H}{\partial y} \frac{\partial \rho_N}{\partial s} \right] ds \quad [13b]$$

### 3. NUMERICAL MODEL OF THE GALVESTON BAY

The Galveston grid is generated through SMS Water Modeling System version 8.0. The model domain extends between longitude 94°20' - 95°13' W and latitude 28°55' - 29°48' N with a grid that consists of 7285 nodes and 13,284 triangular finite elements as shown in Figure 2. The triangular finite element mesh has a resolution from 50m along the channel to 7000m over the shelf and 11 vertical levels in  $\sigma$ -coordinate system arranged as follow:  $\sigma = [-1.000, -0.956, -0.865, -0.689, -0.394, 0.000, 0.394, 0.689, 0.865, 0.956, 1.000]$ . Spherical coordinate system is used for horizontal coordinate system. The grid has one open boundary along the southeast outer boundary, two normal flow boundaries and 17 island/land boundaries.

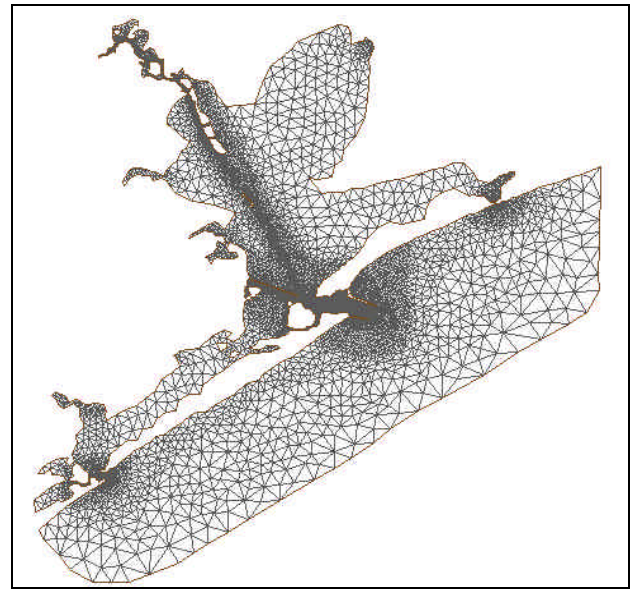


Figure 2. Triangular finite element grid of Galveston Bay.

The ship channel extending from channel entrance in the south to Houston ship channel (HSC) in north end has a nearly uniform 10m contour depth and is 500 – 700 m wide, while the rest of area is shallow water with various depth ranging from 0.2m to 5.0m. The model was driven by two tidal constituent: M2 and K1, in the open boundary, and constant two rivers run off from San Jacinto and Trinity

Rivers as boundary normal flows indicated by arrows in Figure 3. The amplitudes of M2 and K1 tides applied to the open boundary with 33 open boundary nodes vary from 0.09 at the southwest end to 0.16m at the northeast end for M2 tide, and from 0.19m to 0.21m for K1 tide. The freshwater normal flow discharges for San Jacinto and Trinity rivers are constantly arranged to  $Q_{jct} = 150 \text{ m}^3/\text{s}$ . Those values are based on the monthly average of fresh water inflows into the Galveston Bay (GBNEP, 1994), and assumed that both rivers contribute to fresh water discharge equally.

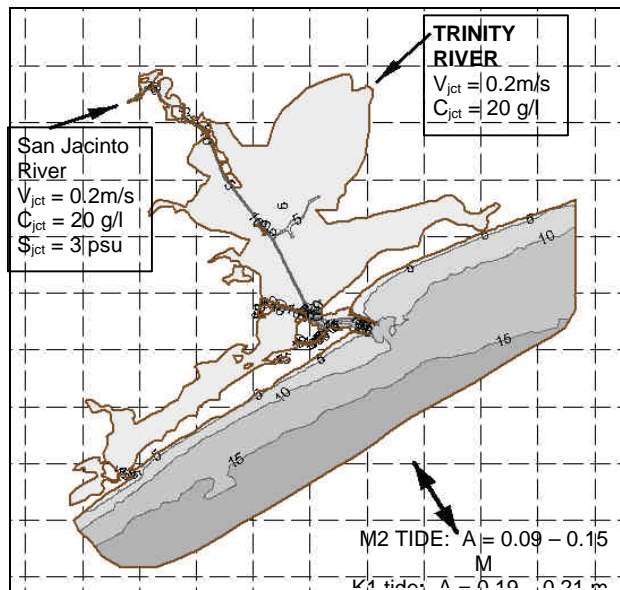


Figure 3. Bathymetric map of Galveston Bay include the south-to-north Houston Ship Channel (HSC). The two main rivers: San Jacinto and Trinity are indicated by arrows.

In this case, the settling velocity was set constant at  $\omega_s = 0.4\text{mm/s}$  which is associated with the typical sediment fall velocity for fine sand, 0.1mm diameter (Kamphuis, 2000). The initial temperature is set uniformly at  $T=19^\circ \text{C}$ . The surface heat flux was calculated using formulation discussed in Helfand et al. (1999) and Hayes et al. (1991). No wind stress is applied in the model. For sediment, initial ambient concentration in the domain is set constant at  $C_o = 2 \text{ g/l}$  ( $=\text{kg/m}^3$ ). Salinity was set constant  $S=35\text{psu}$  in the whole domain. The baroclinic force is generated by the density gradient described in Eq. 14 in which density is determined from salinity and temperature. The normal flow boundaries are defined as essential boundary conditions with constant temperature of  $19^\circ\text{C}$  and concentration  $C_{jct} = C_{trn} = 20\text{g/l}$ . Two different salinity discharge  $S_{jct} = 3\text{psu}$  and  $S_{trn} = 10 \text{ psu}$  are employed at San Jacinto and Trinity Rivers, respectively.

The model was run for 40 days. A mode splitting scheme is used for transport computation where the model solves the two-dimensional, vertically integrated and free surface displacement in external mode, and solves vertical velocity,

salinity, temperature, density and concentration in internal mode. The model used external and internal time steps of 4 seconds and 360 seconds, respectively. The Coriolis force is neglected for simplicity the case.

The inclusion of baroclinic term in the model shows significant difference of three dimensional sediment transport. Figure 4 shows contour distribution of salinity when the baroclinic term is activated. At the initial time of simulation, the saline wedge was strongly developed along the HSC indicated with the front between fresh and saline water in the upper layer propagates much faster than the lower layer, whereas the front in the near bottom layer was left behind (not shown in figure). However, as fresh water influx was in progress moving towards the bay, the process of vertical mixing occurs. Consequently, in the shallow area, the effect of stratification of salinity is not well developed, but instead the salinity become nearly uniform from top to bottom. In the deeper water along the channel, the effect of stratification still exists. Similar process happened in the Trinity Bay, where the salinity stratification was only developed at the initial stage of the model, and then the salinity became well mixed from top to bottom.

After 40 days, as shown in Figure 4, the lower salinity is progressing further in the upper layer ( $\sigma = -0.96$ ; thin lines) than the near bottom layer ( $\sigma = 0.96$ , bold lines) along the ship channel, while in the shallower area the contour of near surface (thin lines) and near bottom (bold lines) salinity are almost coincidence. In the shelf outside the channel entrance the salinity stratification starts to develop which is indicated by the advance of near surface relative to near bottom salinity.

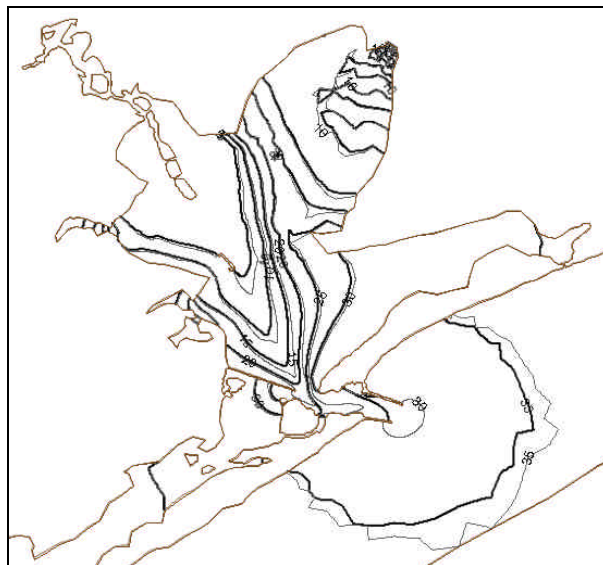


Figure 4. Distribution of salinity after 40 days simulation for near surface (thin line) and near bottom (bold line) layers. Contour index indicates the salinity value in psu.

The hydrodynamic circulation of sediment transport is also successfully developed in the model. It should be noted here that the result of the recent model records only the concentration in the water column based on number of determined sigma layers.

Due to the sediment settling velocity, after a few hours the concentration at the near bottom layers starts to increase, whereas the near surface concentrations tend to decrease. Higher near bottom concentration horizontally occurs mostly near the fresh – saline interface, but the locations of higher concentration progresses southward as the fresh water charge streaming south. This situation typically occurs when there is an existing saline wedge that strengthens the existence of the reverse river flow (Ippen, 1966). In this case, the saline wedge forces the water northward at near bottom decelerating the southward fresh water with high concentration inflow, while near surface the fresh water flows more rapidly due to additional force from the baroclinic term. That saline wedge will resist the sediment at front edge to keep flowing south, and high concentration will occur therefore at this front edge. However, since the baroclinic force is smaller than the normal flow, the location of saline wedge is advancing southward. The length of saline wedge found is about 4.2 km after 40 days simulation.

For comparison between three- and two-dimensional ADCIRC models, another simulation was performed on two-dimensional 2DDI-ADCIRC Transport (Scheffner, 1999) presented in Figure 5a, while the three-dimensional version is depicted in Figure 5b. Both plots were taken after 16 days simulation, and the spread out of concentration of both versions agree. However, it is clearly seen that the contribution of baroclinic term will develop saline wedge (figure is not shown) that decelerates sediment near the salinity front. Consequently, higher sediment concentration will accumulate near bottom behind the front, and higher sediment settling behind the wedge may occur. The concentrations of near bottom increase as high as 40 g/l found in the ship channel, which is associated with the location of leading edge. The situation of high concentration is not clearly shown in the two-dimensional model (Figure 5a), where the sediment distribution is mainly caused by advection and diffusion only without baroclinic term contribution.

After 36 day simulation, in the Galveston Bay where the ship channel is located, near bottom concentration across the channel tends to be higher inside the channel than in the channel flanks (Figure 6). The Ship channel here turns out to be a sediment trap from the river outflow material of San Jacinto River. In the Trinity Bay the near bottom concentration seems distributed uniformly because this bay has nearly uniformly shallow bathymetric depth, and good mixing condition in this area.

Sediment distribution around the channel entrance exhibits specific behavior where unsymmetrical distribution occurs across the entrance (Figure 6). As the flow leaves the Galveston Bay, higher near bottom concentration occurs around the south jetty while the northern jetty receives lower

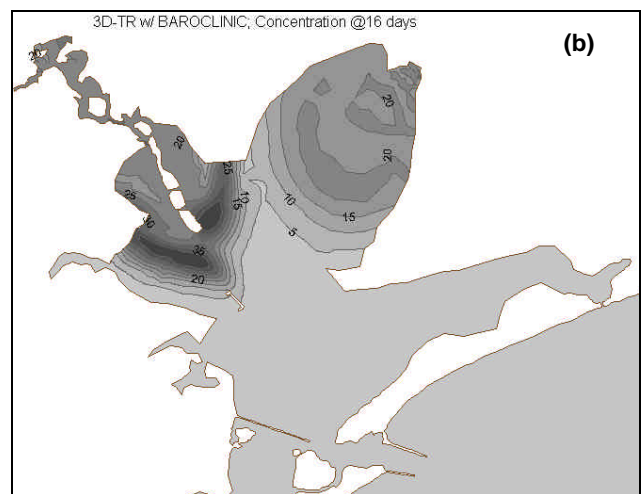
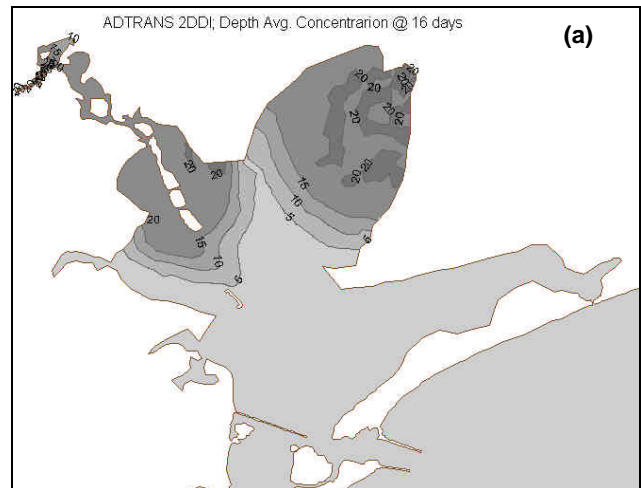


Figure 5. Distribution of sediment concentration after 15 days simulation for (a) 2DDI-ADCIRC Transport version and (b) 3D-ADCIRC Transport with Baroclinic term.

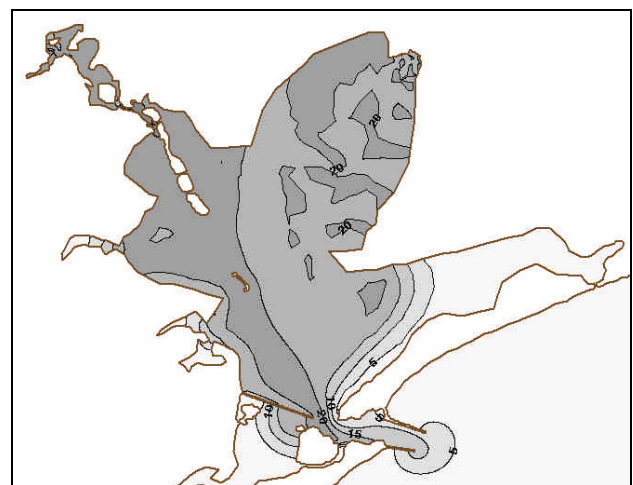


Figure 6. Distribution of sediment concentration after 36 days simulation. Contour index indicates the concentration value in gram/liter.

concentration. Then the higher concentration tends to swing southward as the flow out of concentration runs into the Gulf of Mexico. This behavior may explain the presence of higher deposition sediment in the south jetty of ship channel entrance of the Galveston Bay. Continuous discharge from the Galveston Bay out to Gulf of Mexico may accumulate total suspended sediment around south jetty. Longer simulation may explain more completely the sediment distribution around this area.

#### 4. CONCLUSION

The model simulation performed here demonstrates the ability of developed and newly extended three-dimensional ADCIRC hydrodynamic model to simulate the sediment transport from river inflow. Because of salinity and temperature difference between the saline bay and relatively fresh river water, the effect of baroclinic pressure gradient plays important role in distributing the near bottom sediment. The front zone of fresh-saline water may exhibit or decelerate the sediment flow and trapped them behind the wedge.

In the case of Galveston Bay, the higher concentrations mostly occur along the ship channel that acts as a sediment trap. Prolonged condition may set the sediment at the bottom, and channel-shoaling process will probably exist. The simulation for this bay reveals the higher concentration in the south jetty of channel entrance. This condition need to be investigated further whether the sediment discharge from two rivers used here may contribute to the shoaling process around the jetty. More detail in model setup is needed particularly to achieve this goal.

#### ACKNOWLEDGEMENT

The study described in this paper has been supported in part by the U.S. Environmental Protection Agency through the South and Southwest Hazardous Substance Research Center, the National Science Foundation, and the Texas Engineering Experiment Station at Texas A&M University.

#### REFERENCES:

Fofonoff, N. P., 1985. Physical Properties of Sea Water: A New Salinity Scale and Equation of State for Seawater, *J. Geophys. Res.*, 90(C2), 3332-3342.  
Galveston Bay National Estuary Program (GBNEP), 1994. The State of the Bay. A characterization of the Galveston Bay Ecosystem. Galveston Bay National Estuary Program Publication GBNEP-44. 232pp.  
Grenier, R. R., Jr., Luettich, R. A. Jr., and Westerink, J. J., 1995. A comparison of the nonlinear frictional characteristics of two-dimensional and three-dimensional models of a shallow tidal embayment, *J. Geophys. Res.*, 100(C7), 13,719-13,735.

Hayes, S. P., Chang, P., and McPhaden, M. J. 1991. Variability of Sea Surface Temperature in Eastern Equatorial Pacific during 1986-88. *J. Geophys. Res.*, 96(C6), 10,533 – 10,566.  
Helfand, J. S., Podber D. P., and McCormick, M. J. 1999. Effect of Heat Flux on Thermocline Formation. *Estuarine and Coastal Modeling, Proc. 6<sup>th</sup> Int'l Conference*, Spaulding and Butler (ed.), ASCE, New Orleans, LA.  
Hydroqual, Inc, 1998. "Development and Application of a Modeling Framework to Evaluate Hurricane Impacts on Surficial Mercury Concentrations in Lavaca Bay". Draft Report, Aluminium Co. of America, Point Comfort, Texas.  
Ippen, A. T., 1966. *Estuary and Coastline Hydrodynamics*, McGraw-Hill, New York.  
Kamphuis, J. W., 2000. *Introduction to Coastal Engineering and Management. Advanced Series on Ocean Engineering, Vol. 16*, World Scientific, Singapore.  
Luettich, R. A. Jr. and Muccino, J. 2001. Summary of Vertical Velocity Calculation Methods as Considered for 3D ADCIRC Hydrodynamic Model. Paper presented at ADCIRC Meeting 20-21 Feb 2001, NRL, Stennis, Mississippi.  
Luettich, R. A. Jr., Hu, S., and Westerink J. J. 1994. Development of the Direct Stress Solution Technique for Three-dimensional Hydrodynamic Models using Finite Element. *Int. J. Num. Meth. Fluids*, 19, 295-319.  
Luettich, R. A. Jr., Westerink J. J., and Scheffner, N. W. 1992. ADCIRC: An advanced Three-Dimensional Circulation Model for Shelves, Coasts, and Estuaries. Report 1, Technical Report DRP-92-6, Dredging Res. Prog., USACE, Washington DC.  
Mellor, G. L. 1998. User Guide for a Three-Dimensional, Primitive Equation, Numerical Ocean Model. *Prog. In Atmospheric and Ocean Sciences*, Princeton Univ., Princeton, NJ, 1998  
Mellor, G.L. and Yamada, T. 1982. Development of a turbulence closure model for geophysical fluid problems. *Reviews of Geophysics and Space Physics*, 20, 851-875.  
Muccino, J. C., Gray, W. G., and Foreman, G. G. 1997. Calculation of Vertical Velocity in Three Dimensional, Shallow Water Equation, Finite Elements Model, *Int. J. Num. Meth. Fluids*, 25, 779-802.  
Pandoe, W. and Edge, B. L. 2003. Three-dimensional hydrodynamic model, study cases for quarter annular and idealized ship channel problems, *J. Ocean Engr.*, accepted, Pergamon, U.K.  
Robertson, R., Padman, L., and Levine, M. D. 2001. A Correction of the Baroclinic Pressure Gradient Term in the Princeton Ocean Model. *J. Atmos. Oceanic Technol.*, 18 (6), 1068 – 1075.  
Scheffner, N., 1999. A Large Domain Convection Diffusion Based Finite Element Transport Model. *Estuarine and Coastal Modeling. Proc. 6<sup>th</sup> Intern. Conf.*, Eds. M.L. Spaulding and H. L. Butler, ASCE, pp.194-208, 1999.